NASA/TM—2004-212979

Oxide Ceramic Films Grown on 55Ni-45Ti for NASA and Department of Defense Applications: Unidirectional Sliding Friction and Wear Evaluation

Kazuhisa Miyoshi and Dorothy Lukco
Glenn Research Center, Cleveland, Ohio

Sheldon J. Cytron
U.S. Army Research Laboratory, Development and Engineering Center
Picatinny Arsenal, New Jersey

March 2004

The NASA STI Program Office . . . in Profile

Since its founding, NASA has been dedicated to the advancement of aeronautics and space science. The NASA Scientific and Technical Information (STI) Program Office plays a key part in helping NASA maintain this important role.

The NASA STI Program Office is operated by Langley Research Center, the Lead Center for NASA's scientific and technical information. The NASA STI Program Office provides access to the NASA STI Database, the largest collection of aeronautical and space science STI in the world. The Program Office is also NASA's institutional mechanism for disseminating the results of its research and development activities. These results are published by NASA in the NASA STI Report Series, which includes the following report types:

- TECHNICAL PUBLICATION. Reports of completed research or a major significant phase of research that present the results of NASA programs and include extensive data or theoretical analysis. Includes compilations of significant scientific and technical data and information deemed to be of continuing reference value. NASA's counterpart of peer-reviewed formal professional papers but has less stringent limitations on manuscript length and extent of graphic presentations.

- TECHNICAL MEMORANDUM. Scientific and technical findings that are preliminary or of specialized interest, e.g., quick release reports, working papers, and bibliographies that contain minimal annotation. Does not contain extensive analysis.

- CONTRACTOR REPORT. Scientific and technical findings by NASA-sponsored contractors and grantees.

- CONFERENCE PUBLICATION. Collected papers from scientific and technical conferences, symposia, seminars, or other meetings sponsored or cosponsored by NASA.

- SPECIAL PUBLICATION. Scientific, technical, or historical information from NASA programs, projects, and missions, often concerned with subjects having substantial public interest.

- TECHNICAL TRANSLATION. English-language translations of foreign scientific and technical material pertinent to NASA's mission.

Specialized services that complement the STI Program Office's diverse offerings include creating custom thesauri, building customized databases, organizing and publishing research results . . . even providing videos.

For more information about the NASA STI Program Office, see the following:

- Access the NASA STI Program Home Page at ***http://www.sti.nasa.gov***

- E-mail your question via the Internet to help@sti.nasa.gov

- Fax your question to the NASA Access Help Desk at 301–621–0134

- Telephone the NASA Access Help Desk at 301–621–0390

- Write to:
  NASA Access Help Desk
  NASA Center for AeroSpace Information
  7121 Standard Drive
  Hanover, MD 21076

NASA/TM—2004-212979

Oxide Ceramic Films Grown on 55Ni-45Ti for NASA and Department of Defense Applications: Unidirectional Sliding Friction and Wear Evaluation

Kazuhisa Miyoshi and Dorothy Lukco
Glenn Research Center, Cleveland, Ohio

Sheldon J. Cytron
U.S. Army Research Laboratory, Development and Engineering Center
Picatinny Arsenal, New Jersey

National Aeronautics and
Space Administration

Glenn Research Center

March 2004

This work was sponsored by the Low Emissions Alternative Power Project of the Vehicle Systems Program at the NASA Glenn Research Center.

Available from

NASA Center for Aerospace Information
7121 Standard Drive
Hanover, MD 21076

National Technical Information Service
5285 Port Royal Road
Springfield, VA 22100

Available electronically at http://gltrs.grc.nasa.gov

Oxide Ceramic Films Grown on 55Ni-45Ti for NASA and Department of Defense Applications: Unidirectional Sliding Friction and Wear Evaluation

Kazuhisa Miyoshi and Dorothy Lukco
National Aeronautics and Space Administration
Glenn Research Center
Cleveland, Ohio 44135

Sheldon J. Cytron
U.S. Army Research Laboratory, Development and Engineering Center
Picatinny Arsenal, New Jersey 07806

Summary

An investigation was conducted to examine the friction and wear behavior of the two types of oxide ceramic films furnished by the U.S. Army Research Laboratory, Development and Engineering Center (ARDEC) under Space Act Agreement SAA3–567. These two types of oxide ceramics were grown on 55Ni-45Ti (60 wt% Ni and 40 wt% Ti) substrates: one was a TiO_2 with no other species (designated the B film) and the other was a TiO_2 with additional species (designated the G film). Unidirectional ball-on-disk sliding friction experiments were conducted with the oxide films in contact with sapphire at 296 K (23 °C) in ~50-percent relative humidity laboratory air in this investigation. All material characterization and sliding friction experiments were conducted at the NASA Glenn Research Center. The results indicate that both films greatly improve the surface characteristics of 55Ni-45Ti, enhancing its tribological characteristics. Both films decreased the coefficient of friction by a factor of 4 and increased wear resistance by a two-figure factor, though the B film was superior to the G film in wear resistance and endurance life. The levels of coefficient of friction and wear resistance of both films in sliding contact with sapphire were acceptable for NASA and Department of Defense tribological applications. The decrease in friction and increase in wear resistance will contribute to longer wear life for parts, lower energy consumption, reduced related breakdowns, decreased maintenance costs, and increased reliability.

Introduction

Ceramics, for the most part, do not have inherently good friction properties. For example, coefficients of friction in excess of 0.5 have been reported for silicon carbide sliding on silicon carbide, sapphire sliding on sapphire, silicon nitride sliding on silicon nitride, and silicon nitride sliding on M50 bearing steel (refs. 1 to 3). All of these studies confirm that ceramic tribological components and systems need to be lubricated (ref. 4). This is a significant challenge because the required application temperatures are often higher than the thermal oxidation limits of lubricating oils and even of conventional solid lubricants such as graphite and molybdenum disulfide. This lubrication issue can act as a severe brake in the development of technologies—and indeed, has already done so (ref. 5). For example, gas bearing designs are limited to lower operating temperatures if start and stop are performed under load because, in general, they are dry-rubbing bearings using either a hard/hard combination of materials, such as ceramics with or without a molecular layer of boundary lubricant, or a hard/soft combination using a polymer surface (ref. 6). Therefore, research to develop high-temperature, low-friction ceramics in film and coating form or bulk form is a logical approach to this problem.

Oxide ceramic films and coatings have unique capabilities as mechanical-, chemical-, and thermal-barrier materials in diverse applications, including gas bearings requiring wear resistance and chemical stability at elevated temperatures. In addition, some oxide ceramic films and coatings, such as SiO_2, possess fairly low friction (ref. 7).

This investigation was conducted to examine the friction and wear behavior of oxide ceramic films furnished by the U.S. Army Research Laboratory, Development and Engineering Center (ARDEC) under Space Act Agreement SAA3–567. The primary purpose of this agreement is the technology transfer of the new oxide ceramic films so that they can be evaluated for NASA and Department of Defense applications. Two types of oxide ceramics were applied to 55Ni-45Ti (60-wt% Ni, 40-wt% Ti) substrates: one was a TiO_2 with no other species (designated the B film for convenience), and the other was a TiO_2 with additional metallic species (designated the G film).

Materials

TiO_2 with no other species was formed on 60 nitinol (60 wt% Ni and 40 wt% Ti) using a patented oxide treatment (U.S. Patent 6,422,010). The 60 nitinol metal disks are placed in an air furnace and ramped up to a temperature setting of between 1123 and 1223 K (850 and 950 °C). This is accomplished in approximately 2 hr on the basis of the furnace loading. After this temperature setting is held for approximately 2 hr, the specimens receive a rapid quench into water to harden the surface. The Rockwell hardness level (Rockwell C 54 to C 60) attained is function of the treatment temperature and the rapidity of the water quench. Rockwell C 54 is attained at 1123 K whereas Rockwell C 60 can be reached using a treatment temperature of 1223 K. The cooled specimen is then degreased and the process is repeated to provide a second oxide layer. After this, the oxide surface is polished with diamond paste to provide the reflective, smooth surface finish.

TiO_2 with additional metallic species was formed on 60 nitinol by heating the specimen manually in a MAPP flame. MAPP gas is made by combining methylacetylene-propadiene with liquefied petroleum gas (propane).

Experiments

Materials Characterization

The analytical techniques used to characterize the surface chemistry, morphology, and topography of the oxide ceramic films, substrate, and counterpart material included (1) x-ray photoelectron spectroscopy (XPS) to characterize the surface chemistry and identify the chemical compositions; (2) optical interferometry (optical profilometry without contact) with a profile height resolution of 0.1 nm to determine surface characteristics, such as the topography, roughness, and wear volume loss; (3) scanning electron microscopy (SEM) with energy dispersive spectroscopy (EDS) to determine the morphology and elemental composition of wear surfaces, transferred materials, and wear debris; and (4) Vickers hardness testing to determine the microhardness of the films.

XPS is a surface-sensitive technique that allows for the identification and quantification of elements and trace contaminants found on a surface (approximately 3.0 to 5.0 nm). It is also sensitive to matrix effects, allowing for chemical state information about any elements detected. Varying the takeoff angle of the electrons coming from the sample surface makes it possible to obtain extremely sensitive surface data (<1.5 nm). Depth profiling of layered materials is also possible if ion bombardment of the surface is alternated with elemental analysis. XPS spectra were acquired on a VG Mk II ESCALAB, using Mg K_α

x-rays with an emission current of 20 mA and an accelerating voltage of 15 keV. The base pressure in the analytical chamber was 1×10^{-8} Pa ($N\cdot m^{-2}$). The analyzer operated in the constant analyzer energy mode with 50-eV pass energy, and the spectra were taken with the surface plane normal to the analyzer axis using an aperture of 1 mm by 1 mm. An Ar^{+} ion beam with 4-kV kinetic energy was used to depth profile the specimens. Survey scans were taken of the as-received specimens to identify any trace components, and these were followed by multiplex scans of the individual peak regions. Each of the samples was then lightly sputtered (1.7 nm removed) to remove any adventitious carbon and oxygen that were present on solid surfaces that had been exposed to air and to help identify any trace elements. Depth profiles were then obtained on each of the elements identified in the survey scans.

Friction and Wear Experiment

Unidirectional ball-on-disk sliding friction experiments were conducted at 296 K (23 °C) in ~50-percent relative humidity laboratory air in this investigation. All sliding experiments were conducted with 6-mm-diameter sapphire balls in sliding contact with TiO_2-based films at an initial Hertzian contact pressure of ~0.6 GPa, at a constant speed of 120 rpm, and with a sliding velocity that ranged from 38 to 119 $mm\cdot s^{-1}$ because of the wear track radii involved in the experiments. The friction-and-wear apparatus used in the investigation (fig. 1) was mounted in a chamber. The apparatus can measure friction in air during sliding. The friction force was continuously monitored during the experiments. Wear was quantified by measuring the size of the wear scar and wear track on each specimen after the wear experiment.

Two or three sliding wear experiments were conducted with each material couple at each wear condition. Then, the data were averaged to obtain the wear volume loss of material. The wear volume loss was determined by using the optical profiler without contact or by using SEM.

The wear volume loss of a disk specimen was determined by using noncontact, optical profilometry. This method characterizes and quantifies surface roughness, height distribution, critical dimensions (such as the area and volume of the damaged wear tracks), and topographical features. It has three-dimensional profiling capability with excellent precision and accuracy (e.g., profile heights ranging from ≤1 nm up to 1000 μm with 0.1-nm height resolution). The shape of a surface can be displayed by a computer-generated map developed from digital data derived from a three-dimensional interferogram of the surface. In this investigation, all measurements were made with an effective magnification of × 2.5097 (a × 5 magnification objective and a × 0.5 magnification eyepiece) that profiled an effective field-of-view with a 1.875- by 2.463-mm area and height sampling up to 1000 μm for disk specimens.

The wear volume loss of a ball specimen was determined by measuring the size of the wear scar on the tip of the ball after an experiment. The diameter of the wear area was measured on an SEM photographic print by using electronic digital calipers, SEM image analysis, or optical microscopy image analysis. Then the volume of material that would have been removed was calculated from the average diameter of the circular wear scar.

Hardness Measurement

All indentations were made with a diamond Vickers indenter at a load ranging from 0.1 to 3 N in air at room temperature. The time in contact was 20 s. Each hardness value was the average of five measurements.

Results and Discussion

Surface Chemistry

XPS surface analysis and depth profiling were performed on both films. A survey scan of the as-received surface of the B film (fig. 2(a)) showed it to consist primarily of titanium and oxygen with surface contaminants, such as carbon. The initial analysis of this as-received surface only showed the presence of titanium, oxygen, and carbon. After a light sputter for 1 min, the carbon was gone and only titanium oxide remained (fig. 2(b)). An XPS depth profile was set up to monitor these elements (fig. 3). It can be seen that the titanium concentration and oxygen concentration remained at around 30 and 70 at.%, respectively, as the film was sputtered. Depth profiling indicated that the B film was composed strictly of titanium oxides. Since the oxygen-to-titanium ratio was slightly greater than 2, it seems likely that oxygen was present in forms other than titanium dioxide. The multiplex scans of the individual peak regions indicated that the titanium was not fully oxidized but showed the appearance of a second, less oxidized state, possibly TiO.

The initial survey scan of the as-received surface of the G film (fig. 4(a)) showed mostly carbon and oxygen, along with zinc and nickel. After a 1-min sputter, oxides of zinc, nickel, titanium, and lead, along with carbon and oxygen, were identified on the surface (fig. 4(b)). A depth profile was set up, monitoring these elements (fig. 5). As shown in figure 5, the carbon dropped off quickly (< 5.0 nm), and zinc and nickel decreased in concentration, with a thickness of approximately 20 to 30 nm. A small amount of lead (<2 at.%) was also observed within the top 15 nm of the surface layer. There was an increasing amount of titanium oxides found with increasing depth. At 27 nm in depth, the titanium concentration and oxygen concentration were 25.8 and 63.2 at.%, respectively (also see fig. 4(c)). The multiplex scans of the individual peak regions indicated that the lead was present in two states, possibly PbO and Pb_3O_4. The thin G film was made by heating the specimen manually in a MAPP flame, so the contaminants in the MAPP gas are what we are seeing as Zn and Pb impurities.

Titanium was fully oxidized within the first few tens of nanometers, followed by the appearance of a second, more reduced state of titanium oxide, possibly TiO, deeper into the film.

Microhardness

The average value and standard deviation of the Vickers hardness of the 55Ni-45Ti substrate were 4.48 and 0.11 GPa, respectively, at an indentation load of 3 N. Figure 6 presents the Vickers microhardnesses of the two films as a function of load. At loads between 0.1 and 3 N, no cracks were observed in and around all the Vickers indentations in either the B or G film. The Vickers microhardness of the films was influenced by the indentation load. The hardness of the B film decreased with increasing load and became closer to the hardness of the Ni-Ti substrate (4.48 GPa). On the other hand, the hardness of the G film increased with increasing load and was close to the hardness of the Ni-Ti substrate at higher loads. All the hardness values of the B film were higher than those of the G film. At a load of 0.1 N, the hardness and indentation depth of the B film were 6.61 GPa and 1.04 μm, respectively, whereas those of the G film were 2.85 GPa and 1.62 μm. Note that the hardness of a film should be viewed with caution. Although the indentation depth on the B film at 0.1 N was smaller than the thickness of the B film, the hardness depended on that of the substrate. Especially, the indentation depth on the G film was much greater than the thickness of the G film (~30 nm), the hardness of the G film should be viewed as a reference only.

Coefficient of Friction and Film Durability

Figures 7(a) and (b) present typical friction traces with scattering for the B and G film, respectively, in sliding contact with sapphire as a function of the number of passes up to 1000 passes. The traces in figure 7 show closely spaced irregularities (scatter). In general, the mean value and scatter of the coefficients of friction are susceptible to changes in sliding conditions. For the B film (fig. 7(a)), the height of the scattering is relatively small. The mean coefficient of friction gradually increased as the number of passes increased, and it reached the steady-state coefficient of friction (0.26) at around 500 passes. On the other hand, for the G film, both the mean value and the height of the scatter of the coefficients of friction (fig. 7(b)) strongly depended on the number of passes. After 250 passes, both of the values started to increase as the number of passes increased. The steady-state coefficient of friction was 0.25. However, the mean value and scatter of the coefficient of friction drastically increased after the sapphire broke through the G film. Note that the steady-state coefficient of friction for 55Ni-45Ti in sliding contact with sapphire was 1.1 (table I).

Figure 8 presents a typical friction trace with scattering for the B film in sliding contact with sapphire as a function of the number of passes up to 300 000 passes. In this investigation, the sapphire broke through the B film at around 240 000 passes. We found that the heights of the scatter in the friction trace strongly increased after the sapphire broke through the film, whereas the mean coefficients of friction were almost unchanged before and after this occurred.

When the film wear life (endurance life) was defined as the number of passes at which the mean value or scatter in the coefficient of friction abruptly increased, the average sliding wear lives of the B and G films were approximately 240 000 passes and 260 passes, respectively. The wear life of the B film, because of its greater thickness, was 900 times longer than that of the G film.

Wear Rate and Wear Resistance

Figure 9 presents SEM micrographs of the wear track of the B film in sliding contact with a sapphire ball after 10 000 sliding passes. The SEM micrograph taken at a low magnification shows that the worn surface of the B film was relatively smooth, indicating that the B film was still present. Although closer SEM examination showed that a couple of wear debris particles had chipped off the worn surface, the wear damage was minimal. Like the wear track produced on the B film, the wear scar of the counterpart sapphire ball surface was generally smooth. Closer SEM examination at a higher magnification revealed only very locally smeared, thin patches of transferred materials.

The SEM micrograph of the wear track produced on the G film after 200 sliding passes against a sapphire ball showed that the worn surface was relatively smooth, indicating that the G film was still present. After 10 000 passes, however, both the wear scar on the sapphire ball (fig. 10) and the wear track on the G film (fig. 11) were generally rough. Closer SEM examination at a higher magnification revealed the worn surface of the sapphire and G film, indicating substantial wear damage. The G film had been removed from the wear track, and EDS analysis revealed that the wear track contained predominantly nickel and titanium.

The wear volume losses of the wear tracks produced on the films were quantified using optical profilometry. Then the mean dimensional wear coefficients of the films (specific wear rates), the volume loss of the material removed per unit distance and unit load, were calculated. The average wear rates for the B and G films in sliding contact with sapphire were 6.3×10^{-7} and 1.4×10^{-6} $mm^3\cdot N^{-1}\cdot m^{-1}$, respectively (as shown in fig. 12 and table I). The wear resistance (reciprocal of the dimensional wear coefficient) of the B film was 2 times greater than that of the G film. The wear rate obtained in air at 296 K for the Ni-Ti in sliding contact with sapphire was 4.5×10^{-5} $mm^3\cdot N^{-1}\cdot m^{-1}$. Thus, the wear resistance (reciprocal of the dimensional wear coefficient) of the Ni-Ti was 70 times smaller than that of the B film.

The wear rate of the sapphire ball depended on the counterpart material and its wear rate (as shown in fig. 12 and table I). The higher the wear rate of counterpart material, the greater the wear rate of the sapphire ball. The wear directly related to the chemical reactions, the adhesion, and the physical interactions of the materials couple. The wear rates of sapphire increased in the following order of counterpart materials: B film, G film, and Ni-Ti.

Summary of Results

The surface of the B film consisted primarily of titanium and oxygen with surface contaminants, such as carbon. The B film was composed strictly of titanium oxides. The titanium was not fully oxidized: it showed the appearance of a second, less oxidized state, possibly TiO.

The surficial layer of the G film consisted of oxides of zinc, nickel, titanium, and lead, along with carbon and oxygen. The carbon was present in the top 5.0 nm of the surface layer, and zinc and nickel were present in the top 20 to 30 nm of the surface layer. A small amount of lead (<2 at.%) was present in two states, possibly PbO and Pb_3O_4, within the top 15 nm of the surface layer. Titanium was fully oxidized within the first few tens of nanometers, followed by the appearance of a second, more reduced state of titanium oxide, possibly TiO, deeper into the film.

The hardness of the bare 55Ni-45Ti substrate was 4.48 GPa, which was greater than that of the G film grown on 55Ni-45Ti. The hardness of the B film was higher than that of the G film and 55Ni-45Ti. At a load of 0.1 N, the hardness of the B film was 6.61 GPa at an indentation depth of 1.04 μm, whereas that of the G film was 2.85 GPa at an indentation depth of 1.62 μm. No cracks were observed in either film in and around all the Vickers indentations made at loads between 0.1 and 3 N.

The steady-state coefficients of friction for the B film, G film, and 55Ni-45Ti in sliding contact with sapphire were 0.26, 0.25, and 1.1, respectively. Although the scatter of the coefficients of friction of the B film increased after the sapphire broke through the film at around 240 000 passes, the mean coefficients of friction were almost unchanged before and after this occurred. On the other hand, both the mean value and the scatter of the coefficients of friction of the G film drastically increased after the sapphire broke through at around 260 passes. The wear life of the B film, because of its greater film thickness, was 900 times longer than that of the G film.

The average wear rates for the B and G films in sliding contact with sapphire were 6.3×10^{-7} and 1.4_10^{-6} $mm^3\cdot N^{-1}\cdot m^{-1}$, respectively. The wear resistance (reciprocal of the dimensional wear coefficient) of the B film was 2.2 times greater than that of the G film. The wear rate obtained in air at 296 K for the Ni-Ti in sliding contact with sapphire was 4.5×10^{-5} $mm^3\cdot N^{-1}\cdot m^{-1}$. Thus, the wear resistance values (reciprocal of the dimensional wear coefficient) of the B and G films were 71 and 32 times greater than that of the 55Ni-45Ni.

The wear rate of sapphire depends on the counterpart material and its wear rate. The higher the wear rate of the counterpart material, the greater the wear rate of the sapphire ball. The wear rates of sapphire increased in the following order of counterpart materials: B film, G film, and Ni-Ti.

Concluding Remarks

The surface characteristics of 55Ni-45Ti are much improved by both films, enhancing the tribological characteristics. The films decreased the coefficient of friction by a factor of 4 and increased the wear resistance by a two-figure factor, though the wear resistance and endurance life of the B film were superior to those of the G film. The levels of coefficient of friction and wear resistance of both films in sliding contact with sapphire were acceptable for NASA and Department of Defense tribological

applications. The decrease in friction and increase in wear resistance will contribute to longer wear parts lives, lower energy consumption, reduced related breakdowns, decreased maintenance costs, and increased reliability.

References

1. Buckley, D.H.; and Miyoshi, K.: Tribological Properties of Structural Ceramics. Structural Ceramics, J.B. Wachtman, Jr., ed., Treatise on Materials Science and Technology, vol. 29, Academic Press, Inc., Boston, 1989, pp. 293–365.
2. Sutor, P.: Tribology of Silicon Nitride and Silicon Nitride-Steel Pairs. Ceram. Eng. Sci. Proc., vol. 5, 1984, pp. 461–469.
3. Sikra, J.C., et al.: Sliding Friction and Wear of Selected Ceramics. Am. Ceram. Soc. Bull., vol. 58, 1974, pp. 581–582.
4. Sliney, H.E., et al.: Tribology of Selected Ceramics at Temperatures to 900 °C. Ceram. Engrg. Sci. Proc., vol. 7, nos. 7–8, 1986, pp. 1039–1051.
5. Jost, H.P.: Tribology—Origin and Future. Wear, vol. 136, 1990, pp. 1–17.
6. Khonsari, M.M.; Matsch, L.A.; and Shapiro, W.: Gas Bearings. Handbook of Lubrication and Tribology, vol. 3, Monitoring, Materials, Synthetic Lubricants, and Applications, E.R. Booser, ed., CRC Press, Inc., Boca Raton, 1994, pp. 553–575.
7. Holmberg, K.; and Matthews, A.: Coatings Tribology. Tribology Series, vol. 28, D. Dowson, ed., Elsevier, Amsterdam, 1994.

TABLE I.—STEADY-STATE COEFFICIENT OF FRICTION, DIMENSIONAL WEAR COEFFICIENT, AND WEAR LIFE OF FILMS IN SLIDING CONTACT WITH SAPPHIRE IN AIR AT 296 K

Material	Steady-state coefficient of friction	Dimensional wear coefficient, $mm^3 \cdot N^{-1} \cdot m^{-1}$	Films wear life, passes
B film (TiO_2 alone)	~0.26	6.3×10^{-7}	~240 000
G film (TiO_2 with additional species)	~0.25	1.4×10^{-6}	~260
Ni-Ti	1.1	4.5×10^{-5}	--------

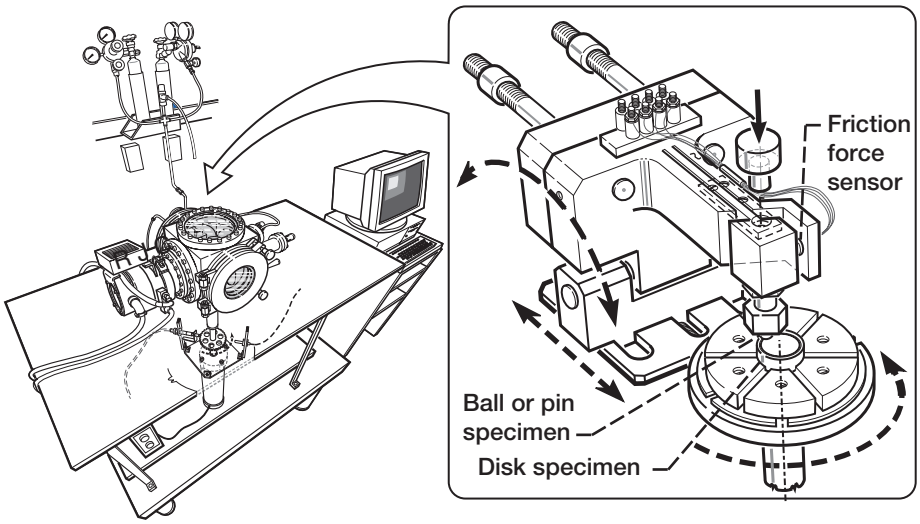

Figure 1.—Unidirectional ball-on-disk sliding friction apparatus.

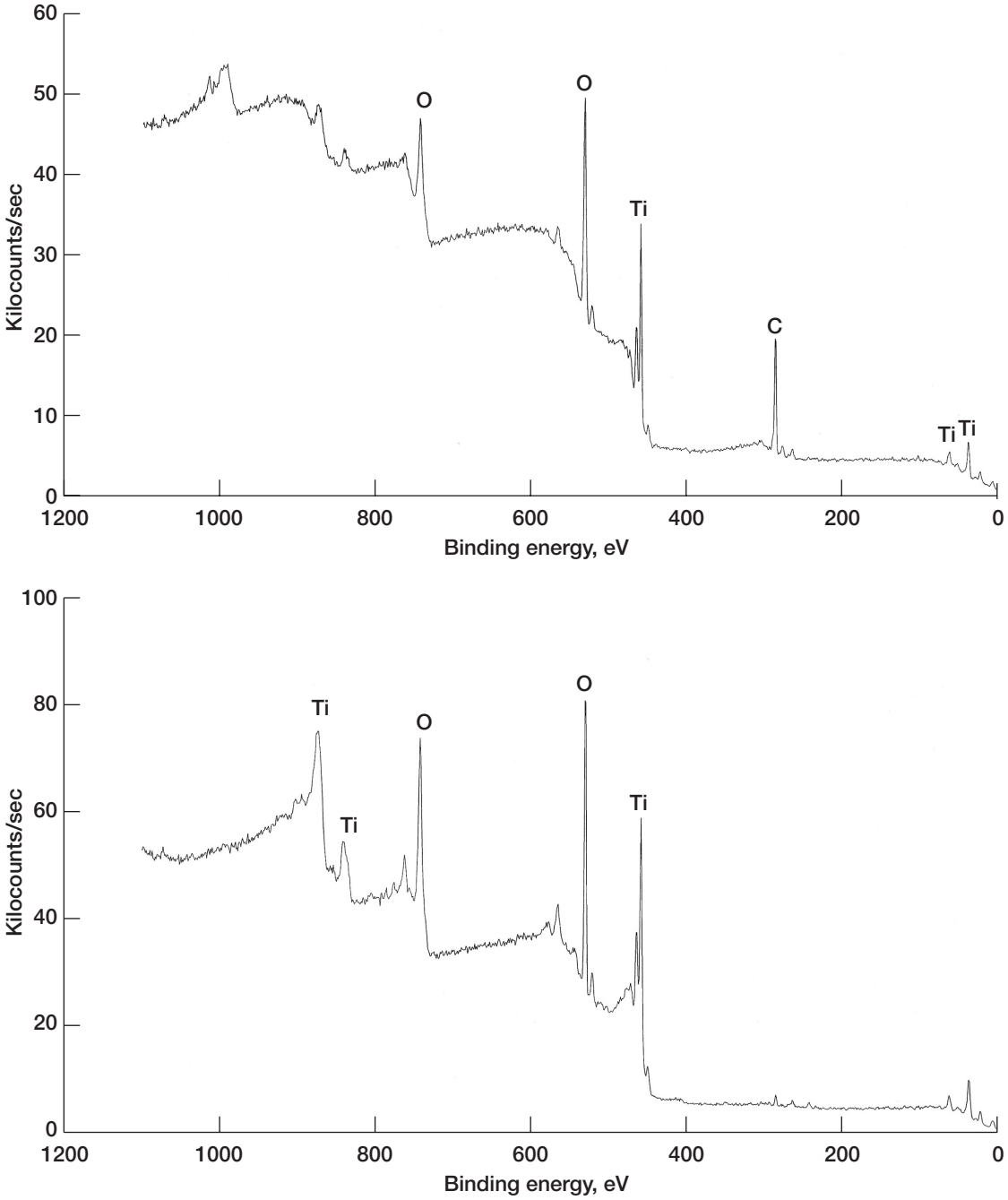

Figure 2.—X-ray photoelectron spectroscopy (XPS) survey spectra of TiO_2 specimen (B film). (a) As-received surface. (b) Ion-sputtered surface (sputtering for 1 min).

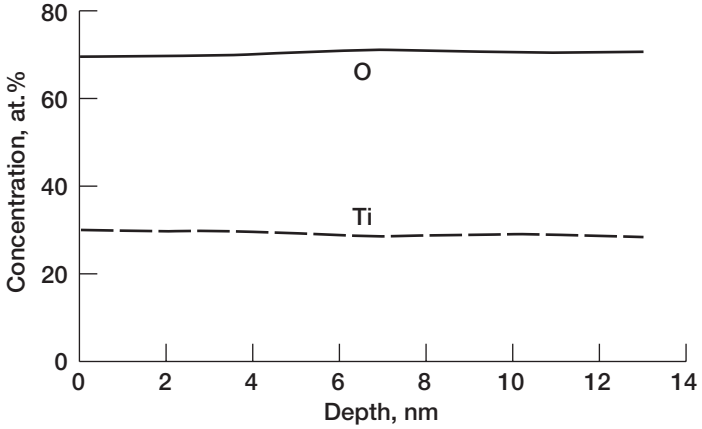

Figure 3.—XPS depth profile of TiO_2 specimen (B film).

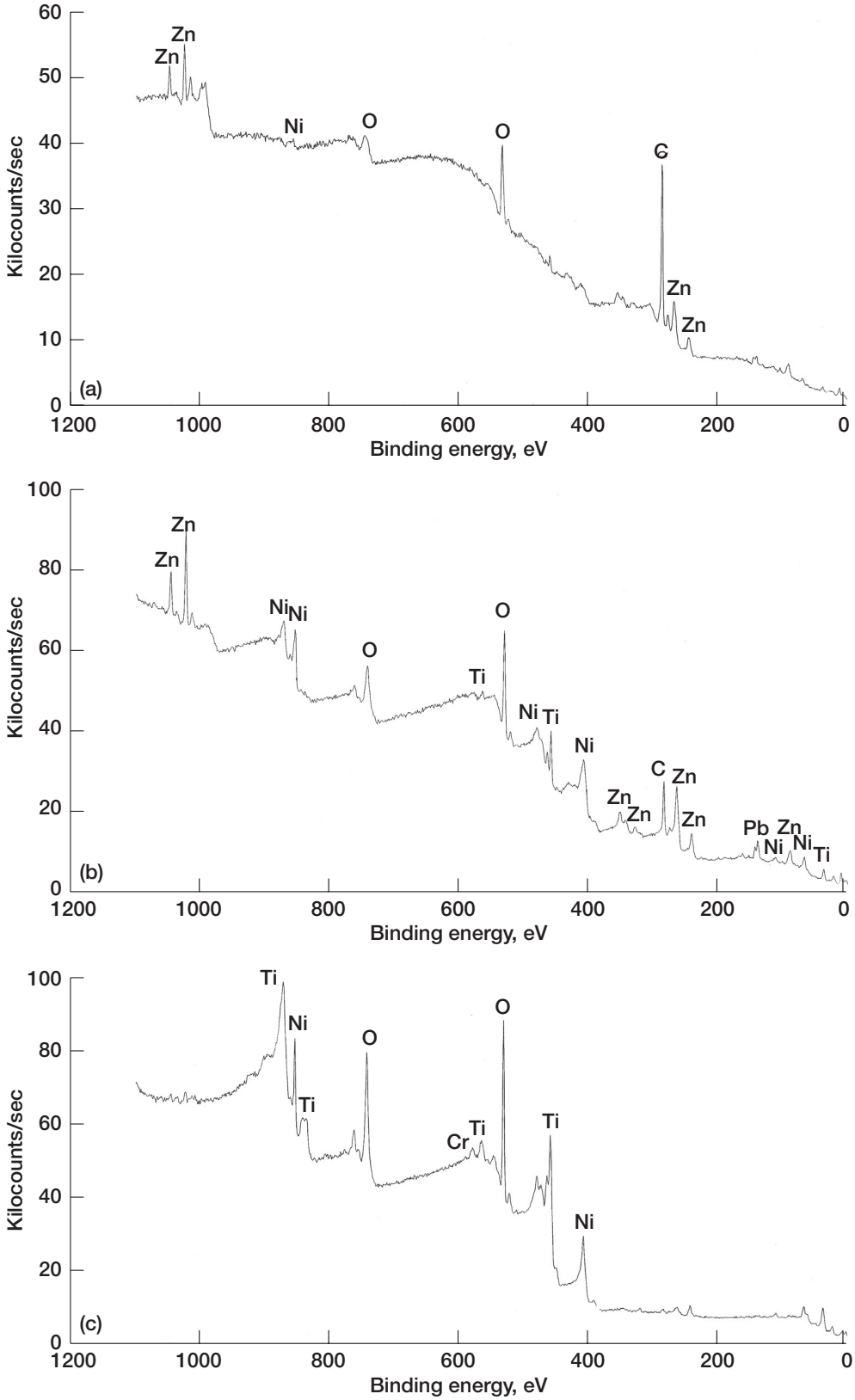

Figure 4.—X-ray photoelectron spectroscopy (XPS) survey spectra of TiO_2 specimen with additional species (G film). (a) As-received surface. (b) Ion-sputtered surface (sputtering for 1 min). (c) Ion-sputtered surface at a depth of 27 nm.

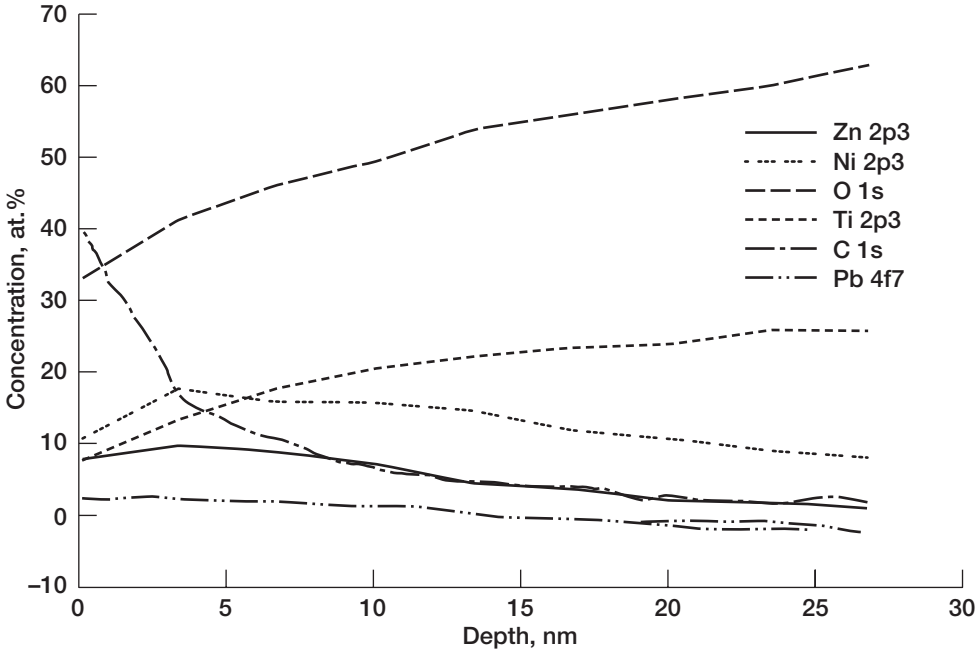

Figure 5.—XPS depth profile of TiO_2 specimen with additional species (G film).

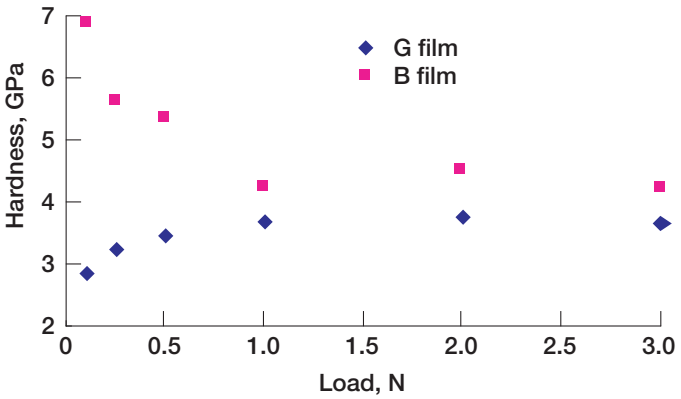

Figure 6.—Vickers microhardness of TiO_2 specimen (B film) and TiO_2 specimen with additional species (G film) as a function of indentation load.

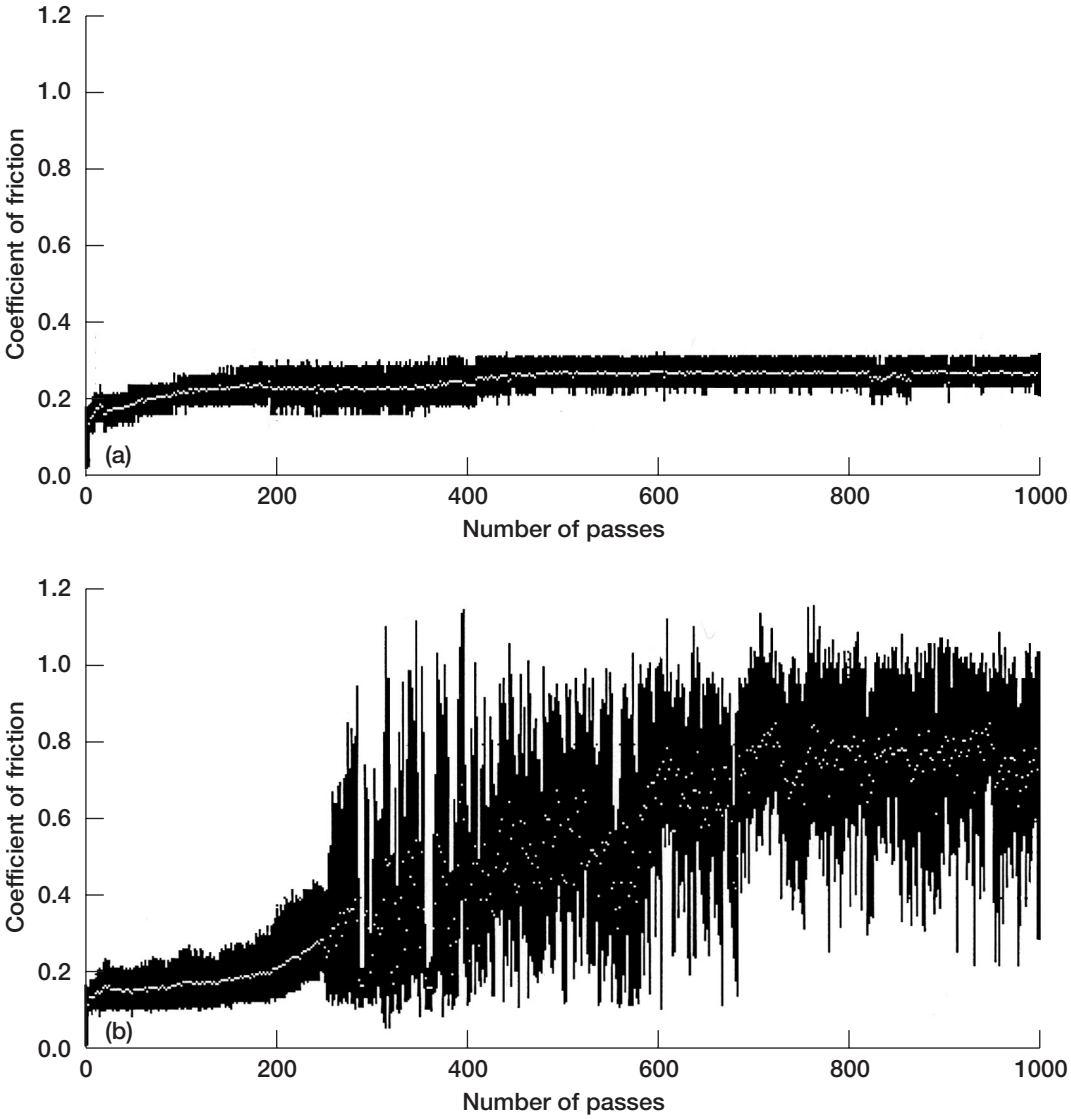

Figure 7.—Coefficient of friction for specimens in sliding contact with sapphire as a function of the number of passes to 1000 passes in air at 296 K. (a) TiO_2 specimen (B film). (b) TiO_2 specimen with additional species (G film).

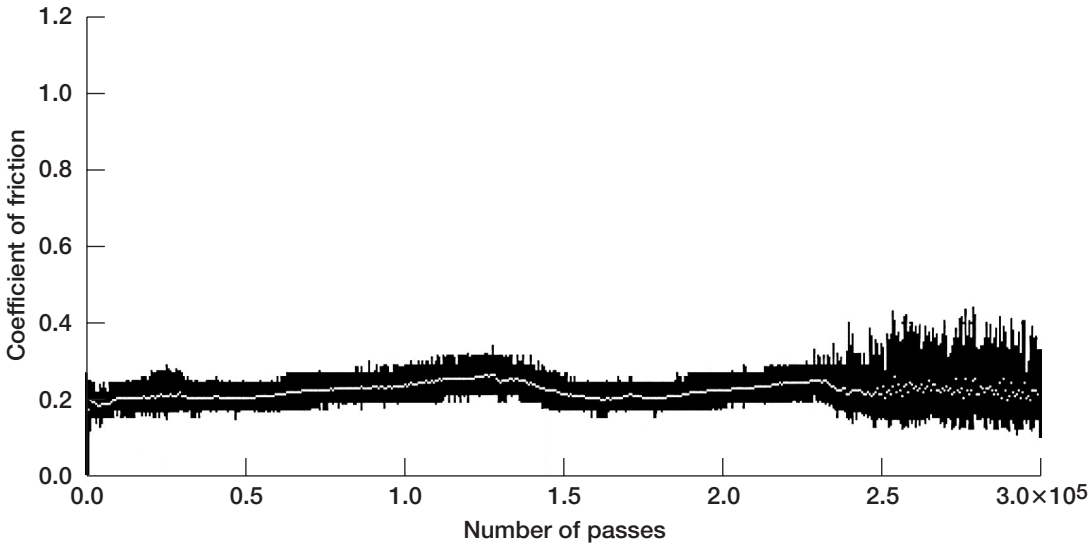

Figure 8.—Coefficient of friction for TiO_2 specimen (B film) in sliding contact with sapphire as a function of the number of passes to 300 000 passes in air at 296 K.

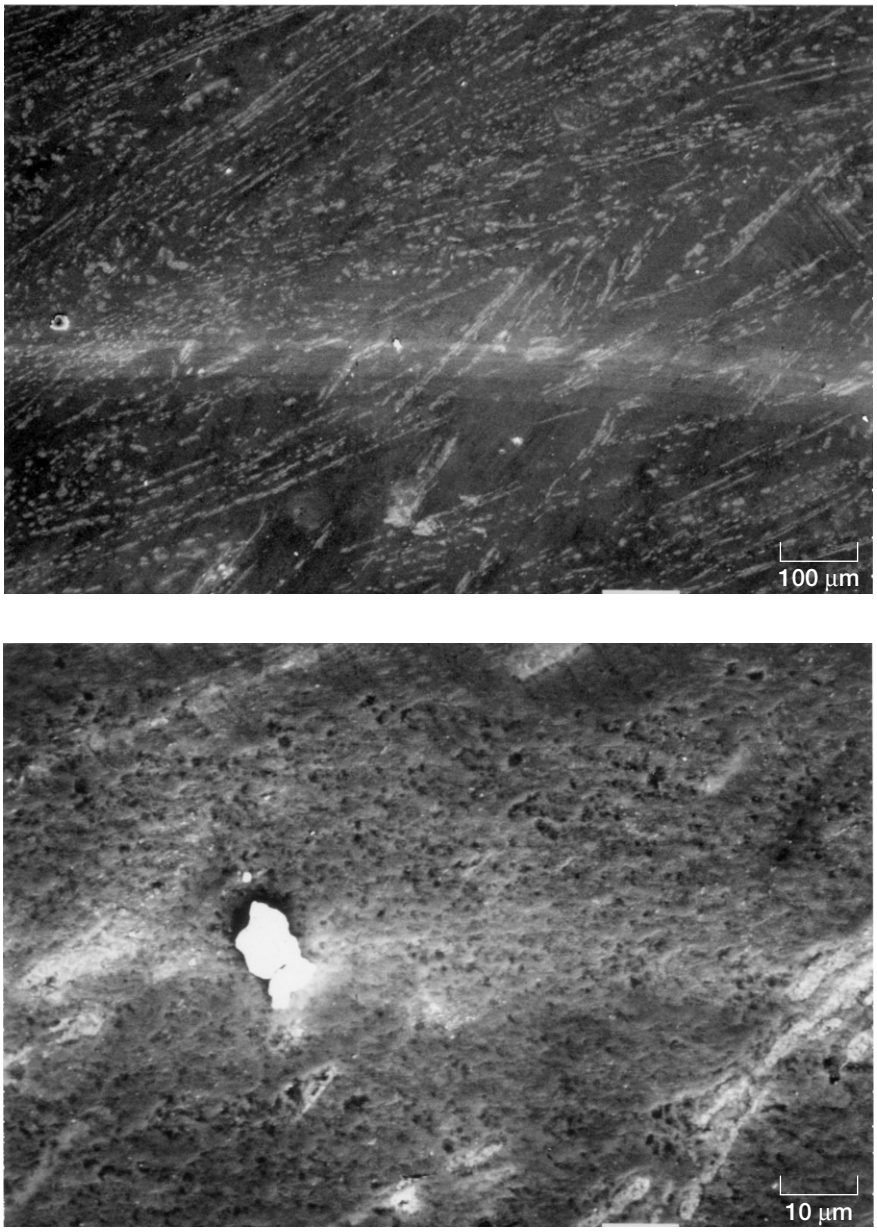

Figure 9.—Wear track produced on TiO_2 specimen (B film) in sliding contact with sapphire for 10 000 passes at 296 K in air. (a) Low magnification. (b) High magnification.

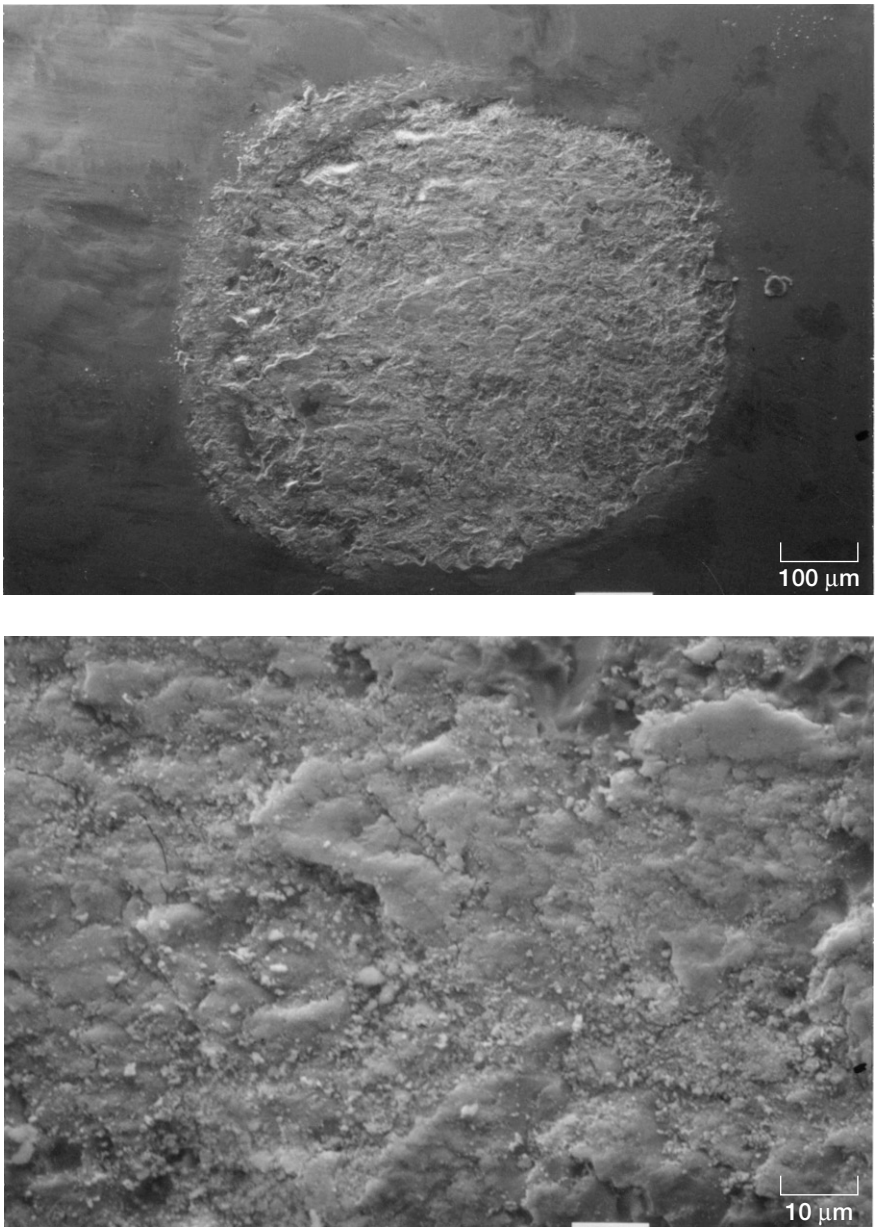

Figure 10.—Wear scar produced on sapphire in sliding contact with TiO_2 specimen with additional species (G film) for 10 000 passes at 296 K in air. (a) Low magnification. (b) High magnification.

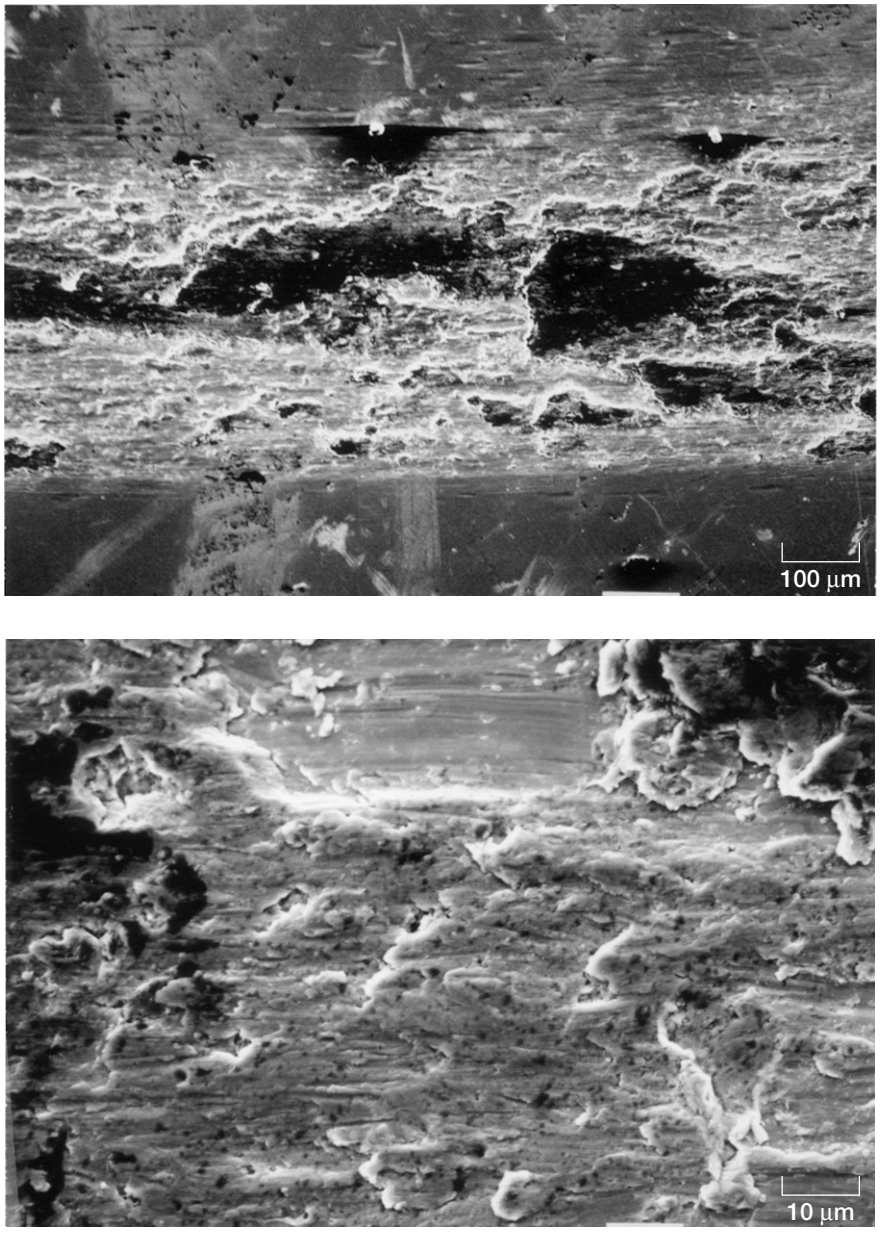

Figure 11.—Wear track produced on TiO_2 specimen with additional species (G film) in sliding contact with sapphire for 10 000 passes at 296 K in air. (a) Low magnification. (b) High magnification.

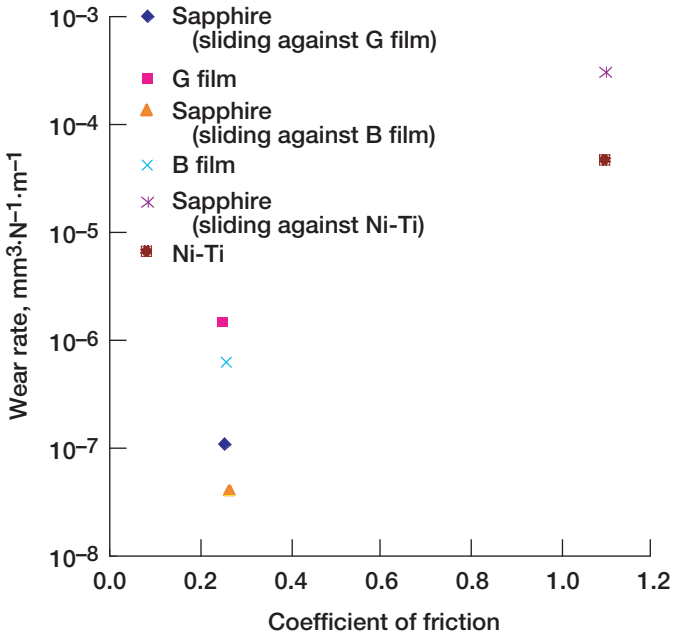

Figure 12.—Dimensional wear coefficient (wear rate) and coefficient of friction of TiO_2 specimen (B film), TiO_2 specimen with additional species (G film), and counterpart sapphire.

REPORT DOCUMENTATION PAGE

Form Approved
OMB No. 0704-0188

1. AGENCY USE ONLY (*Leave blank*)	2. REPORT DATE	3. REPORT TYPE AND DATES COVERED
	March 2004	Technical Memorandum

4. TITLE AND SUBTITLE

Oxide Ceramic Films Grown on 55Ni-45Ti for NASA and Department of Defense Applications: Unidirectional Sliding Friction and Wear Evaluation

5. FUNDING NUMBERS

WBS–22–708–04–04

6. AUTHOR(S)

Kazuhisa Miyoshi, Dorothy Lukco, and Sheldon J. Cytron

7. PERFORMING ORGANIZATION NAME(S) AND ADDRESS(ES)

National Aeronautics and Space Administration
John H. Glenn Research Center at Lewis Field
Cleveland, Ohio 44135–3191

8. PERFORMING ORGANIZATION REPORT NUMBER

E–14316

9. SPONSORING/MONITORING AGENCY NAME(S) AND ADDRESS(ES)

National Aeronautics and Space Administration
Washington, DC 20546–0001

10. SPONSORING/MONITORING AGENCY REPORT NUMBER

NASA TM—2004-212979

11. SUPPLEMENTARY NOTES

Kazuhisa Miyoshi and Dorothy Lukco, NASA Glenn Research Center; and Sheldon J. Cytron, U.S. Army Research Laboratory, Development and Engineering Center, Picatinny Arsenal, New Jersey 07806. Responsible person, Kazuhisa Miyoshi, organization code 5160, 216–433–6078.

12a. DISTRIBUTION/AVAILABILITY STATEMENT

Unclassified - Unlimited
Subject Category: 27 Distribution: Nonstandard

Available electronically at http://gltrs.grc.nasa.gov

This publication is available from the NASA Center for AeroSpace Information, 301–621–0390.

12b. DISTRIBUTION CODE

13. ABSTRACT ***(Maximum 200 words)***

An investigation was conducted to examine the friction and wear behavior of the two types of oxide ceramic films furnished by the U.S. Army Research Laboratory, Development and Engineering Center (ARDEC) under Space Act Agreement SAA3–567. These two types of oxide ceramics were grown on 55Ni-45Ti (60 wt% Ni and 40 wt% Ti) substrates: one was a TiO_2 with no other species (designated the B film) and the other was a TiO_2 with additional species (designated the G film). Unidirectional ball-on-disk sliding friction experiments were conducted with the oxide films in contact with sapphire at 296 K (23 °C) in ~50-percent relative humidity laboratory air in this investigation. All material characterization and sliding friction experiments were conducted at the NASA Glenn Research Center. The results indicate that both films greatly improve the surface characteristics of 55Ni-45Ti, enhancing its tribological characteristics. Both films decreased the coefficient of friction by a factor of 4 and increased wear resistance by a two-figure factor, though the B film was superior to the G film in wear resistance and endurance life. The levels of coefficient of friction and wear resistance of both films in sliding contact with sapphire were acceptable for NASA and Department of Defense tribological applications. The decrease in friction and increase in wear resistance will contribute to longer wear life for parts, lower energy consumption, reduced related breakdowns, decreased maintenance costs, and increased reliability.

14. SUBJECT TERMS

TiO_2; Ni-Ti; Sapphire; Wear; Friction; Oxide ceramic films

15. NUMBER OF PAGES

24

16. PRICE CODE

17. SECURITY CLASSIFICATION OF REPORT	18. SECURITY CLASSIFICATION OF THIS PAGE	19. SECURITY CLASSIFICATION OF ABSTRACT	20. LIMITATION OF ABSTRACT
Unclassified	Unclassified	Unclassified	